Nanoscale

Accepted Manuscript
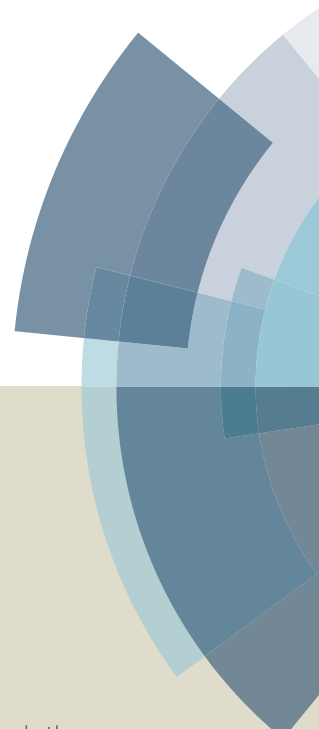
Volume 1 | Number 1 | Jan 2013 | Pages 1–100

Nanoscale
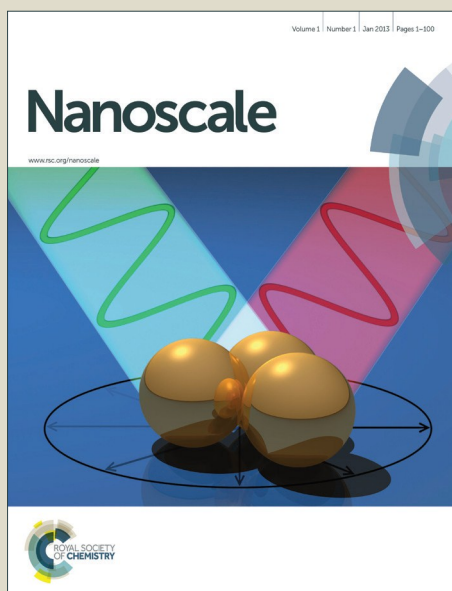
www.rsc.org/nanoscale

ROYAL SOCIETY
OF CHEMISTRY

Journal Name

ARTICLE

Identification of a positive-Seebeck-coefficient exohedral fullerene

Nasser Almutlaq[‡a,c], Qusiy Al-Galiby[‡a,b,d], Steven Bailey[‡a,b] and Colin Lambert*[‡a,b]

If fullerene-based thermoelectricity is to become a viable technology, then fullerenes exhibiting both positive and negative Seebeck coefficients are needed. C_{60} is known to have a negative Seebeck coefficient and therefore in this paper we address the challenge of identifying a positive-Seebeck-coefficient fullerene. We investigated the thermoelectric properties of single-molecule junctions of the exohedral fullerene $C_{50}Cl_{10}$ connected to gold electrodes and found that it indeed possesses a positive Seebeck coefficient. Furthermore, in common with C_{60}, the Seebeck coefficient can be increased by placing more than one $C_{50}Cl_{10}$ in series. For a single $C_{50}Cl_{10}$, we find S=+8 μV/K and for two $C_{50}Cl_{10}$'s in series we find S=+30 μV/K. We also find that the $C_{50}Cl_{10}$ monomer and dimer have power factors of 0.5×10^{-5} W/m.K^2 and 6.0×10^{-5} W/m.K^2 respectively. These results demonstrate that exohedral fullerenes provide a new class of thermoelectric materials with desirable properties, which complement those of all-carbon fullerenes, thereby enabling the boosting of the thermovoltage in all-fullerene tandem structures.

Introduction

Tuning the thermoelectric properties of single molecules is of great interest, because they are potential building blocks for new materials with enhanced electrical and thermal functionality. When a single molecule is connected across a nanogap between two electrodes, whose temperatures differ by an amount ΔT, the resulting voltage difference ΔV=-S ΔT is determined by the Seebeck coefficient (S) of the junction. This molecular-scale Seebeck effect has stimulated a recent outpouring of fundamental research aimed at controlling and increasing the efficiency of organic thermoelectric materials, using combinations of mechanical, electrostatic, chemical and electrochemical gating[1-23].

As an example of such control, recent scanning tunneling microscope (STM) experiments[10] measured the conductance and thermopower of C_{60} molecules and found that compared with a single C_{60}, the Seebeck coefficient could be almost doubled by placing C_{60}s in series to form dimers. These experiments suggest that thin molecular films of fullerenes may be excellent thermoelectric materials. However to build a usable all-fullerene device, it will necessary to boost the thermovoltage in a tandem arrangement, by placing materials with Seebeck coefficients of opposite signs in series. Since C_{60} is found to have a negative Seebeck coefficient, in the present paper we address the challenge of identifying a fullerene with a positive Seebeck coefficient. Recent experiments on the endohedral fullerene[13] $Sc_3N@C_{80}$ demonstrated that the Seebeck coefficient of this material could be either positive or negative, depending on the applied pressure. Although this compound does not meet our challenge, because the sign of the Seebeck coefficient is variable, it does suggest that

chemical modification may solve the problem of identifying positive-Seebeck-coefficient fullerenes. Therefore in the present paper we examine for the first time the possibility of controlling thermoelectricity in exohedral fullerenes. In particular, we study the exohedral decachlorofullerene $C_{50}Cl_{10}$, which is chemically stable and was first fabricated in milligram quantities in 2004[24,25] . Our aim is to explore the potential for thermoelectricity of molecular junctions formed from one or two decachlorofullerenes attached to gold electrodes and to determine if their properties can be controlled by mechanical gating.

To compute the thermoelectric properties of such junctions, we note that in the linear-response regime, the electric current I and heat current $\dot{Q}$ passing through a device is related to the voltage difference ΔV and temperature difference ΔT by [1]

$$\begin{pmatrix} I \\ \dot{Q} \end{pmatrix} = \frac{2}{h} \begin{pmatrix} e^2 L_0 & \dfrac{e}{T} L_1 \\ e L_1 & \dfrac{1}{T} L_2 \end{pmatrix} \begin{pmatrix} \Delta V \\ \Delta T \end{pmatrix} \tag{1}$$

where T is the reference temperature and

$$L_n = \int_{-\infty}^{\infty} (E - E_F)^n \, T(E) \left(-\frac{\partial f(E,T)}{\partial E} \right) dE \tag{2}$$

In this expression e=-|e| is the electronic charge, $T(E)$ is the

a. Department of physics, Lancaster University, Lancaster LA1 4YB, UK.
b. Quantum Technology Centre, Lancaster University, Lancaster LA1 4YB, UK
c. Department of Physics, Northern Border University, Saudi Arabia.
d. Department of physics, College of Education, Al-Qadisiyah University, Diwaniyah, 58002, IRAQ
‡ Authors contributed equally.
*Corresponding author: c.lambert@lancaster.ac.uk, qusiyalgaliby@gmail.com
†Electronic Supplementary Information (ESI) available: [details of any supplementary information available should be included here]. See DOI: 10.1039/x0xx00000x

ARTICLE

transmission coefficient for electrons of energy E, passing through the molecule from one electrode to the other and $f(E,T)$ is Fermi distribution defined as $f(E,T) = [e^{(E-E_F)/k_BT} + 1]^{-1}$ where k_B is Boltzmann's constant.

When $\Delta T = 0$, equation (1) yields for the electrical conductance

$G = (\frac{I}{\Delta V})_{\Delta T=0}$,

$$G = \frac{2e^2}{h}L_0 \qquad (3)$$

Similarly when $I = 0$, equation (1) yields for the Seebeck coefficient

$S = -(\frac{\Delta V}{\Delta T})_{I=0}$,

$$S = \frac{-1}{|e|T}\frac{L_1}{L_0} \qquad (4),$$

whereas the Peltier coefficient (∏), and the electronic contribution to the thermal conductance (κ_e) are given by

$$\Pi = \frac{-1}{|e|}\frac{L_1}{L_0} \qquad (5)$$

$$\kappa_e = \frac{2}{hT}\left(L_2 - \frac{(L_1)^2}{L_0}\right) \qquad (6)$$

From the above expressions, the electronic thermoelectric figure ZT_e =S^2GT/κ_e is given by

$$ZT_e = \frac{(L_1)^2}{L_0L_2 - (L_1)^2} \qquad (7)$$

For E close to E_F, if $T(E)$ varies approximately linearly with E on the scale of k_BT then these formulae take the form[1, 2]

$$G(T) \approx \left(\frac{2e^2}{h}\right)T(E_F), \qquad (8)$$

$$S(T) \approx -\alpha|e|T\left(\frac{d\,lnT(E)}{dE}\right)_{E=E_F}, \qquad (9)$$

$$\kappa_e \approx \alpha TG, \qquad (10)$$

where $\alpha = \left(\frac{k_B}{e}\right)^2\frac{\pi^2}{3} = 2.44.10^{-8}$ WΩK^{-2} is the Lorentz number. Equation (9) demonstrates that S is enhanced by increasing the slope of ln $T(E)$ near $E=E_F$.
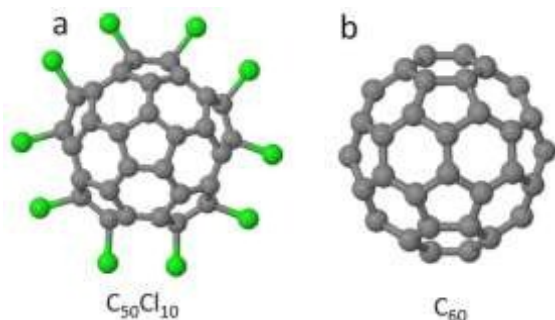

Figure 1. Optimized geometries for exohedral-fullerene (C$_{50}$Cl$_{10}$)[24,25] left and fullerene (C60) right.

Methods

Figure 1 shows a comparison between, the fullerene C$_{60}$ (right) and the exohedral-fullerene C$_{50}$Cl$_{10}$ (left), which consists of a smaller fullerene C$_{50}$ surrounding by 10 equatorial chlorines. To undertake a comparative study of

their thermoelectric properties, when placed between two gold electrodes, we used the density functional theory (DFT) code SIESTA[26] which employs Troullier-Martins pseudopotentials[27] to represent the potentials of the atomic cores, and a local atomic-orbital basis set. A double-zeta polarized basis set was used for all atoms and the generalized gradient approximation (GGA-PBE) for the exchange and correlation functionals [28,29]. The Hamiltonian and overlap matrices were calculated on a real-space grid defined by a plane-wave cut-off of 150 Ry. Each molecule was relaxed to the optimum geometry until the forces on the atoms were smaller than 0.02 eV/Å and in case of the isolated molecules, a sufficiently-large unit cell was used.

Results and Discussion

For the dimers, we varied the distance between two molecules from 1.2 to 5 Å and computed their binding energy as a function of distance. As shown in figure 2, for a C$_{60}$ dimer, the optimum separation of the C$_{60}$s is 3.5 Å and the binding energy is (~-0.05 eV), while for the C$_{50}$Cl$_{10}$ dimer, the optimum C$_{50}$Cl$_{10}$ separation is 3.2 Å and the binding energy is (~-0.03 eV).

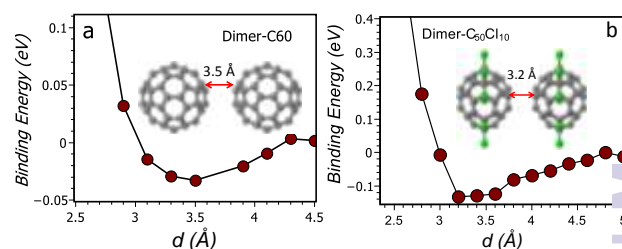**Figure 2.** DFT calculation of the binding energy as a function of distance between (Left) two C60 and (Right) two C$_{50}$Cl$_{10}$. The inset figures show the optimum structure for the dimer.

Next, each relaxed molecule or dimer was placed between two gold (111) electrodes, as shown in Figures 3a and 3b. After geometry relaxation, the distance between each molecule and the gold electrode was found to be 2.2 Å and the charge transferred between the chlorine atoms and fullerene C$_{50}$ is shown in tables S1 of the SI. Figures 3a and 3b, show optimum configurations of single and dimer C$_{60}$ junctions, in which the distance between two C$_{60}$s is d =3.5 Å and the distance between the C$_{60}$s and electrodes is r=2.2 Å. To compute their thermoelectric properties, we used the quantum transport code Gollum[30], which combines the Hamiltonian provided by the DFT code SIESTA with a Green's function scattering formalism. Figure 3d shows the transmission coefficient $T(E)$ as a function of energy E for the junctions in Figures 3a and 3b.
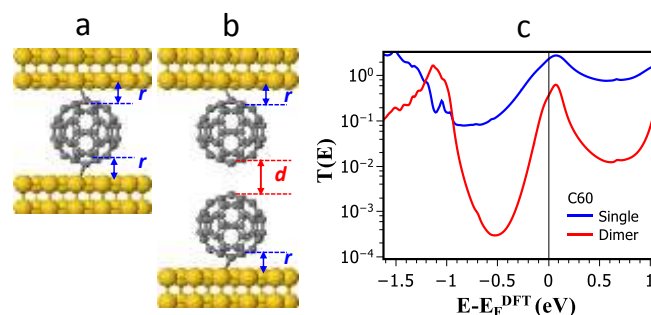

Figure 3. Left panel shows an example of an optimized junction configuration for the systems containing (a) single C60 and (b) a C60 dimer placed between two gold electrodes. Right panel, (c) shows a DFT calculation of their transmission

Journal Name

ARTICLE

coefficients $T(E)$ as a function of energy E relative to the DFT-predicted Fermi energy E_F^{DFT}.

For both the monomer and the dimer, in agreement with ref [10], electrons near the Fermi energy transmit through the tail of the LUMO. Furthermore the dimer transmission (red line) is much smaller than that of the monomer, due to the increase in length of the molecular bridge, leading to a higher slope at the Fermi energy and a higher thermopower for the dimer.

Figure 4a and 4b show the corresponding $C_{50}Cl_{10}$ junctions, whose optimum dimer separation is d=3.2 Å and optimum distance between the $C_{50}Cl_{10}$s and electrodes is r=2.2 Å. Figure 4c shows the transmission coefficient $T(E)$ of the monomer (blue) and dimer (red) and as expected the transmission of the dimer is lower than that of the monomer. Figure 5 shows a comparison between the transmission coefficients and corresponding room-temperature electrical conductances of the $C_{50}Cl_{10}$ and C_{60} monomers and dimers, while Figures 6a-6d show the comparison between their room-temperature Seebeck coefficients (thermopower) S and power factors (σS^2).
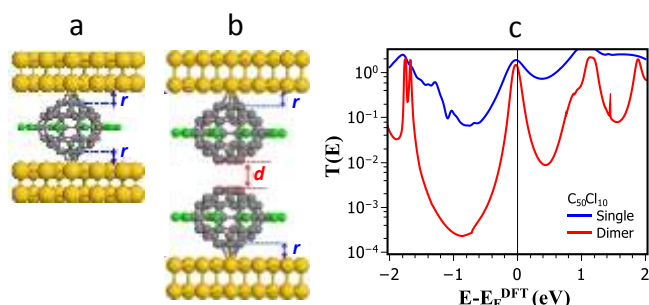

Figure 4. Left panel shows an example of an optimized junction configuration for the systems containing (a) single and (b) dimer fullerene-$C_{50}Cl_{10}$ placed between two gold electrodes. Right panel, (c) shows DFT calculation of transmission coefficient as a function of energy for the structures in Figures 4a and 4b.
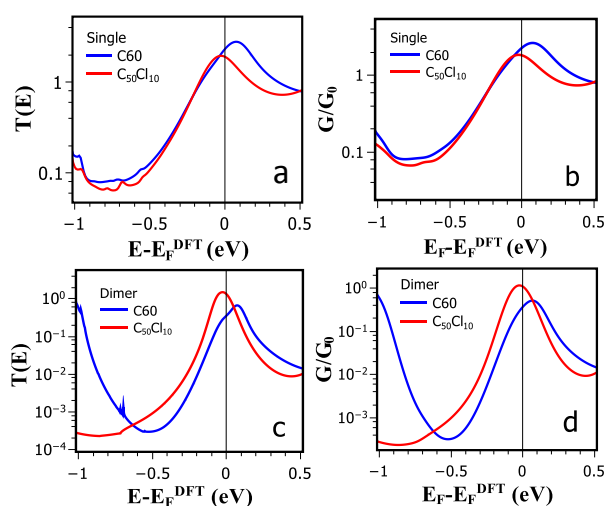

Figure 5. The left column, (Figs a and c) show the of transmission coefficients $T(E)$ between the monomers and dimers in Figures 3 and 4. The right column (Figs b and d) shows their room-temperature electrical conductance (G).
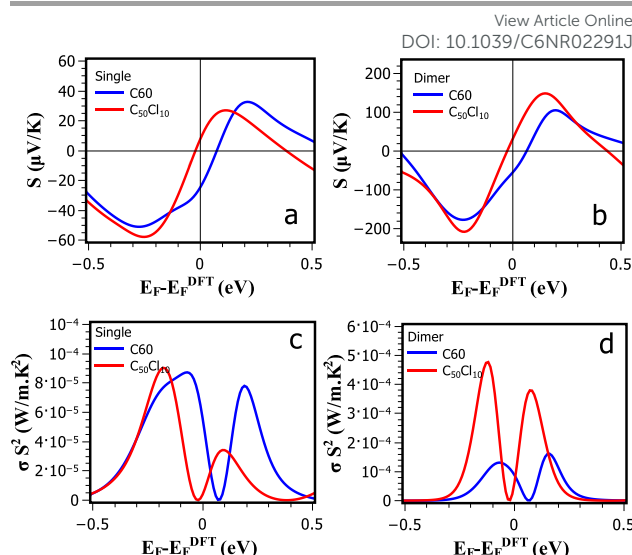
Figure 6. The left column, Figures (a and c) show the room-temperature Seebeck coefficient (thermopower S) and power factor (σS^2) over a range of Fermi energies E_F relative to the DFT-predicted Fermi energy E_F^{DFT} for the monomers in Figures 3a and 4a. The right column, (Figs b and d) shows the room-temperature Seebeck coefficient and power factor (σS^2) for the dimers in Figures 3b and 4b.

The optimum separation of d= 3.2 Å for the $C_{50}Cl_{10}$ dimer and d= 3.5 Å for the C_{60} dimer is chosen for illustrative purposes. In the STM experiment of ref [10], in which the conductance and Seebeck coefficient of a C_{60} dimer was measured, one C_{60} molecule was located on the gold substrate and the other was attached to the STM tip. The distance between them was then varied by varying the position of the STM tip and many hundreds of curves of conductance and Seebeck coefficient versus d were obtained. These curves all differ, because the tip shape, the motion of the tip and the orientations of the molecules vary from measurement to measurement. Since these details are not known, this variation cannot be calculated. Nevertheless as an indication of how transport properties depend on the dimer separation d, figure S3 shows transmission curves for various values of d.

It is well-known[1] that DFT can give an inaccurate value for the Fermi energy and therefore Figures 6a-6c show results for a range of Fermi energies E_F relative to the DFT-predicted Fermi energy E_F^{DFT}. Figure 6a demonstrates that both the magnitude and sign of Seebeck coefficient S is changed by replacing the C_{60} with $C_{50}Cl_{10}$. For example at the DFT-predicted Fermi energy E_F^{DFT}, the Seebeck coefficient of single C_{60} is -21 µV/K and for C_{60} dimer, it increases to -56 µV/K. On the other hand the Seebeck coefficient of the single $C_{50}Cl_{10}$ is +8 µV/K and while for $C_{50}Cl_{10}$ dimer, it increases to +30 µV/K. This increase occurs, because moving from the monomer to the dimer decreases the transmission coefficient at the centre of the HOMO-LUMO gap and since the value of T(E) near the LUMO resonance remains close to unity for both the monomer and the dimer, the slope of the transmission coefficient is larger for the latter. Consequently, the Seebeck coefficient is increased.

For a bulk material, the power factor P is defined by as $P = S^2 \sigma$, where σ is the electrical conductivity. The notion of conductivity is not applicable to transport through single molecules, but to compare with

ARTICLE

Journal Name

literature values for bulk materials, we define $\sigma = GL/A$, where L and A are equal to the length and the cross-sectional area of the molecule respectively. In what follows, for single (dimer) C_{60} the values L=1.13 (2.12) nm and A=2.1 nm^2 are used, whereas for single (dimer) $C_{50}Cl_{10}$ we assign values L=1 (1.85) nm and A=2.1 nm^2. From the results of Figure 6a and 6b, the temperature dependence of the power factors $P = S^2GL/A$ computed using the DFT-predicted Fermi energy are shown in Figure 7c and 7d. These results show that C_{60} monomer and dimer have room-temperature factors of 8.8×10^{-5} W/m.K^2 and 6.3×10^{-5} W/m.K^2 respectively, whereas the $C_{50}Cl_{10}$ monomer and dimer have power factors of 0.5×10^{-5} W/m.K^2 and 6.0×10^{-5} W/m.K^2 respectively.
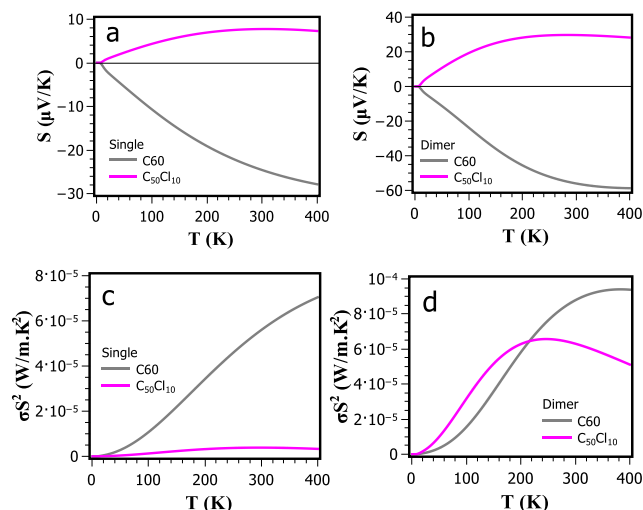

Figure 7. The left column (Figs. a and c) show the Seebeck coefficients *S* and power factors σS^2 as a function of temperature at DFT-predicted Fermi energy E_F^{DFT} for the monomers in Figures 3a and 4a. The right column, (Figs. b and d) show the Seebeck coefficient and power factors for the dimers in Figures 3b and 4b.

Conclusion

In conclusion, we have demonstrated that the exohedral fullerene $C_{50}Cl_{10}$ provides a thermoelectric material with a positive Seebeck coefficient of opposite sign to that of C_{60}. Furthermore, in common with C_{60}, the Seebeck coefficient can be increased by placing more than one $C_{50}Cl_{10}$ in series. For a single $C_{50}Cl_{10}$, we find *S*=+8 μV/K and for two $C_{50}Cl_{10}$'s in series we find *S*=+30 μV/K. These are comparable with the Seebeck coefficients of pristine C_{60}, which we predict to be *S*=-21 μV/K and *S*=-56 μV/K for a C_{60} monomer and C_{60} dimer respectively. Fullerenes smaller than C_{60} are predicted to have unusual electronic, magnetic, and mechanical properties that arise mainly from the high curvature of their molecular surface[31-37]. Our paper demonstrates that thermoelectricity should be added to this list of fascinating properties and that exohedral fullerenes provide a new class of thermoelectric materials with desirable properties, which complement those of all-carbon fullerenes.

The field of molecular thermoelectrics is in its infancy and ongoing studies are needed to highlight how chemical modifications of molecules can be used to tune the thermopower and reverse its sign. $C_{50}Cl_{10}$ is only one of a large number of available exohedral fullerenes and it remains to be seen what levels of performance are attainable. For $C_{50}Cl_{10}$, the change in sign arises because the Fermi energy is located above the LUMO resonance, whereas in C_{60}, it is located below the LUMO resonance. The geometrical and electronics structure $C_{50}Cl_{10}$ is very different from that of C_{60} and

therefore it is not possible to consider a smooth change, which connects the electronic structure of one with the other. For the future it would be of interest to study exhohedral fullerenes obtained by adding eg metal atoms to the outside of the cage, without changing the number of carbon atoms. Since the Seebeck coefficient is an intrinsic property, studies of single molecules inform the design of thin film materials formed from monolayer of multi-layers of molecules. The increase in Seebeck coefficient for the dimer compared with the monomer suggests that performance can be increased by increasing the number of layers in such molecular films, at least until the film thickness reaches the inelastic scattering length. The value of this length is not known for fullerene films, but at room temperature, it can be as much as 3nm in monomer, dimer and trimer porphyrin molecules of in OPEs[38,39].

References

[1] C. J. Lambert, "Basic concepts of quantum interference and electron transport in single-molecule electronics," Chem. Soc. Rev., vol. 44, no. 4, pp. 875–888, 2015.

[2] K. Baheti, J. a. Malen, P. Doak, P. Reddy, S. Y. Jang, T. D. Tilley, A. Majumdar, and R. a. Segalman, "Probing the chemistry of molecular heterojunctions using thermoelectricity," Nano Lett., vol. 8, no. 2, pp. 715–719, 2008.

[3] S. K. Yee, J. A. Malen, A. Majumdar, and R. A. Segalman, "Thermoelectricity in Fullerene–Metal Heterojunctions," Nano Lett., vol. 11, no. 10, pp. 4089–4094, 2011.

[4] S. K. Lee, T. Ohto, R. Yamada, and H. Tada, "Thermopower of benzenedithiol and C60 molecular junctions with Ni and Au electrodes.," Nano Lett., vol. 14, no. 9, pp. 5276–80, 2014.

[5] J. Malen, P. Doak, and K. Baheti, "Identifying the length dependence of orbital alignment and contact coupling in molecular heterojunctions," Nano Lett., vol. 9, no. 3, pp. 1164–1169, 2009.

[6] A. Tan, J. Balachandran, S. Sadat, V. Gavini, B. D. Dunietz, S.-Y. Jang, and P. Reddy, "Effect of length and contact chemistry on the electronic structure and thermoelectric properties of molecular junctions.," J. Am. Chem. Soc., vol. 133, no. 23, pp. 8838–41, 2011.

[7] J. Balachandran and P. Reddy, "End-group-induced charge transfer in molecular junctions: effect on electronic-structure and thermopower," J. Phys. Chem. Lett., vol. 3, no. 15, pp. 1962–1967, 2012.

[8] J. R. Widawsky, W. Chen, H. Vázquez, T. Kim, R. Breslow, M. S. Hybertsen, and L. Venkataraman, "Length-dependent thermopower of highly conducting Au-C bonded single molecule junctions," Nano Lett., vol. 13, no. 6, pp. 2889–2894, 2013.

Journal Name

ARTICLE

[9] W. B. Chang, C. Mai, M. Kotiuga, J. B. Neaton, G. C. Bazan, and R. A. Segalman, "Controlling the Thermoelectric Properties of Thiophene-Derived Single-Molecule Junctions," Chem. Mater., vol. 26, no. 24, pp. 7229–7235, Nov. 2014.

[10] C. Evangeli, K. Gillemot, E. Leary, M. T. González, G. Rubio-Bollinger, C. J. Lambert, and N. Agraït, "Engineering the thermopower of C60 molecular junctions," Nano Lett., vol. 13, no. 5, pp. 2141–2145, 2013.

[11] Y. Kim, W. Jeong, K. Kim, W. Lee, and P. Reddy, "Electrostatic control of thermoelectricity in molecular junctions.," Nat. Nanotechnol., vol. 9, no. 11, pp. 881–5, 2014.

[12] Víctor M García-Suárez, Colin J Lambert, David Zs Manrique andThomas Wandlowski, "Redox control of thermopower and figure of merit in phase-coherent molecular wires," Nanotechnology 25 205402 (2014)

[13] L. Rincón-García, A. K. Ismael, C. Evangeli, I. Grace, G. Rubio-Bollinger, K. Porfyrakis, N. Agraït, and C. J. Lambert, "Molecular design and control of fullerene-based bi-thermoelectric materials," Nature Mater. 15, 289–293 (2016

[14] A. Ismael, I. Grace, and C. Lambert, "Increasing the thermopower of crown-ether-bridged anthraquinones," Nanoscale, 2015.

[15] A. Shakouri, "Thermoelectric power factor for electrically conductive polymers," Eighteenth Int. Conf. Thermoelectr. Proceedings, ICT'99 (Cat. No.99TH8407), no. c, pp. 402–406, 1999.

[16] Al-Galiby, Q. H.; Sadeghi, H.; Algharagholy, L. A.; Grace, I.; Lambert, C.J."Tuning the thermoelectric properties of metallo-porphyrins" Nanoscale, 8, (4), 2428-2433 2016.

[17] P. Reddy, S.-Y. Jang, R. A. Segalman, and A. Majumdar, "Thermoelectricity in Molecular Junctions," Science (80-.)., vol. 315, no. 5818, pp. 1568–1571, 2007.

[18] J. a. Malen, S. K. Yee, A. Majumdar, and R. a. Segalman, "Fundamentals of energy transport, energy conversion, and thermal properties in organic-inorganic heterojunctions," Chem. Phys. Lett., vol. 491, no. 4–6, pp. 109–122, 2010.

[19] J. a. Malen, P. Doak, K. Baheti, T. D. Tilley, A. Majumdar, and R. a. Segalman, "The nature of transport variations in molecular heterojunction electronics," Nano Lett., vol. 9, no. 10, pp. 3406–3412, 2009.

[20] J. R. Widawsky, P. Darancet, J. B. Neaton, and L. Venkataraman, "Simultaneous determination of conductance and thermopower of single molecule junctions," Nano Lett., vol. 12, no. 1, pp. 354–358, 2012.

[21] H. Sadeghi, S. Sangtarash, and C. J. Lambert, "Oligoyne Molecular Junctions for Efficient Room Temperature Thermoelectric Power Generation," Nano Lett., vol. 15, no. 11, pp. 7467–7472, Oct. 2015.

[22] David Zsolt Manrique, Qusiy Hibbeb Al-Galiby, Wenjing Hong, Colin J Lambert "A new approach to materials discovery for electronic and thermoelectric properties of single-molecule junctions" Nano Lett. 16, 1308–1316 2016

[23] Algharagholy, L. A.; Al-Galiby, Q.; Marhoon, H. A.; Sadeghi, H.; Abduljalil, H. M.; Lambert, C. J. "Tuning thermoelectric properties of graphene/boron nitride heterostructures" Nanotechnology 26, (47), 475401 2015

[24] Xie, S.-Y.; Gao, F.; Lu, X.; Huang, R.-B.; Wang, C.-R.; Zhang, X.; Liu, M.-L.; Deng, S.-L.; Zheng, L.-S. Science 2004, 304, (5671), 699-699.

[25] Chen, Zhongfang. "The smaller fullerene C50, isolated as C50Cl10." Angewandte Chemie International Edition 43.36 (2004): 4690-4691.

[26] Soler, José M., et al. "The SIESTA method for ab initio order-N materials simulation." Journal of Physics: Condensed Matter 14.11 (2002): 2745.

[27] Troullier, Norman, and José Luís Martins. "Efficient pseudopotentials for plane-wave calculations." Physical review B 43.3 (1991): 1993.

[28] Perdew, John P., Kieron Burke, and Matthias Ernzerhof. "Generalized gradient approximation made simple." Physical review letters 77.18 (1996): 3865.

[29] Hammer, B. H. L. B., Lars Bruno Hansen, and Jens Kehlet Nørskov. "Improved adsorption energetics within density-functional theory using revised Perdew-Burke-Ernzerhof functionals." Physical Review B 59.11 (1999): 7413.

[30] Ferrer, Jaime, et al. "GOLLUM: a next-generation simulation tool for electron, thermal and spin transport." New Journal of Physics 16.9 (2014): 093029.

[31] K. M. Kadish, R. S. Ruoff, Eds., Fullerene: Chemistry, Physics and Technology (Wiley, New York, 2002).

[32] Guo, Ting, et al. "Uranium Stabilization of C~ 2~ 8: A Tetravalent Fullerene." Science 257.5077 (1992): 1661-1664.

[33] Kroto, H. W. "The stability of the fullerenes Cn, with n= 24, 28, 32, 36, 50, 60 and 70." Nature 329.6139 (1987): 529-531.

[34] Piskoti, C., J. Yarger, and A. Zettl. "C36, a new carbon solid." Nature 393.6687 (1998): 771-774.

[35] Koshio, Akira, et al. "A preparative scale synthesis of C36 by high-temperature laser-vaporization: purification and identification of C36H6 and C36H6O." Journal of the American Chemical Society 122.2 (2000): 398-399.

[36] Koshio, Akira, et al. "In situ laser-furnace TOF mass spectrometry of C36 and the large-scale production by arc-discharge." The Journal of Physical Chemistry B 104.33 (2000): 7908-7913.

[37] Heath, James R. "Fullerenes: C60's smallest cousin." Nature 393.6687 (1998): 730-731.

[38] Sedghi, G.; García-Suárez, V. M.; Esdaile, L. J.; Anderson, H. L.; Lambert, C. J.; Martín, S.; Bethell, D.; Higgins, S. J.; Elliott, M.; Bennett, N. "Long-range electron tunnelling in oligo-porphyrin molecular wires." Nat. Nanotechnol. 2011, 6, 517.

[39] Zhao, X.; Huang, C.; Gulcur, M.; Batsanov, A. S.; Baghernejad, M.; Hong, W.; Bryce, M. R.; Wandlowski, T. "Oligo(aryleneethynylene)s with Terminal Pyridyl Groups: Synthesis and Length Dependence of the Tunnelling to Hopping Transition in Single-Molecule Conductances." Chem. Mat.2013, 25, 4340.